

Recombination characteristics of minority carriers near the $\text{Al}_x\text{O}_y/\text{GaAs}$ interface using the light beam induced current technique

H. Gebretsadik, K. Zhang, K. Kamath, X. Zhang, and P. Bhattacharya^{a)}

Department of Electrical Engineering and Computer Science, Solid-State Electronics Laboratory, University of Michigan, Ann Arbor, Michigan 48109-2122

(Received 27 June 1997; accepted for publication 26 October 1997)

The light beam induced current (LBIC) technique was used to characterize the interface formed by the wet oxidation of AlAs and $\text{Al}_x\text{Ga}_{1-x}\text{As}$ ($x=0.98$ and 0.95). LBIC scans were used to calculate the diffusion lengths of minority carriers both in the bulk and near these interfaces; and the corresponding interface recombination velocities were estimated. The interface recombination velocity at the oxide/semiconductor interface is 3.13×10^5 cm/s for AlAs, and 1.90×10^4 cm/s for $\text{Al}_{0.98}\text{Ga}_{0.02}\text{As}$. It is found that the addition of gallium in the AlAs can significantly improve this property. © 1997 American Institute of Physics. [S0003-6951(97)02452-2]

The thermal oxidation of high Al content AlGaAs layers in water vapor at elevated temperatures forms a stable oxide suitable for use in optoelectronic and electronic devices.¹ An advantage of this wet-oxidation process is that the AlGaAs layer may be selectively oxidized, especially compared to GaAs, making it possible to “bury” the oxidized layers using lateral diffusion in multilayer structures. This process has been effectively used in vertical-cavity surface-emitting lasers (VCSEL) using lattice-matched AlGaAs and GaAs layers, for enhanced electrical and optical confinement.^{2,3} In addition, this oxide has been used in various other electronic devices including, as a gate-insulator in AlGaAs–GaAs field effect transistors (FETs)⁴ and as a buffer insulator in the current GaAs on insulator (GOI) technology.⁵

The electrical properties of these devices are affected by generation and recombination at the oxide/semiconductor interface. In VCSELs, it is imperative to understand how carrier injection into the active region is altered by recombination centers at the oxide aperture. Much study has been done on the structural and mechanical stability of devices utilizing this oxide;⁶ and it has been determined that VCSELs with current apertures formed by the partial lateral oxidation of AlGaAs are far more robust and reliable than those by AlAs. The electronic and structural properties of the selectively oxidized AlAs/GaAs interface have also been examined in detail using time-resolved photoluminescence measurements on multilayer structures and transmission electron microscopy (TEM) diffraction pattern micrographs.⁷ To date, no direct comparison of the oxidized AlAs/GaAs and $\text{Al}_x\text{Ga}_{1-x}\text{As}/\text{GaAs}$ (for $x < 1$) interface recombination properties has been made. We are presenting a quantitative approach to this study by measuring the lifetime of minority carriers in the vicinity of the oxide/semiconductor interface and by estimating the surface recombination velocities near the GaAs/ $\text{Al}_x\text{Ga}_{1-x}\text{As}$ interface for $x=1$, 0.98 , and 0.96 , using the light beam induced current (LBIC) technique.^{8–13}

LBIC is an established method for characterizing minority-carrier diffusion lengths and recombination velocities both in the bulk, at discontinuities such as those encountered in grain boundaries, at regrown interfaces,^{14,15} and

heterointerfaces.⁸ In the technique, scanning the vicinity of a reverse-biased p - n junction or Schottky junction with a laser beam spot and relating the photocurrent response to the distance between the excitation point and the junction will yield the minority carrier diffusion lengths both in the bulk and at the interface.

To perform this study, we have grown three layer structures as shown in Figs. 1(a)–1(c) by molecular beam epitaxy (MBE). Structure A consists of a $1 \mu\text{m}$ n -GaAs ($5 \times 10^{16} \text{cm}^{-3}$) layer, followed by a 500 \AA AlAs and a $1 \mu\text{m}$ n -GaAs, grown on $n+$ GaAs substrate. Structures B and C consist of $1 \mu\text{m}$ n -GaAs, followed by a 500 \AA $\text{Al}_x\text{Ga}_{1-x}\text{As}$ ($x=0.98$ and 0.95) and a $2 \mu\text{m}$ n -GaAs layer. Note that the thickness of the oxide is kept low in order to avoid delamination of the diodes during lapping and polishing. The grown layers were mesa etched prior to the partial lateral oxidation of the AlGaAs layer. The samples were then placed in a furnace tube at $450 \text{ }^\circ\text{C}$. Water vapor was supplied to the tube by flowing nitrogen at 75 sccm through water heated at $90 \text{ }^\circ\text{C}$. The lateral oxidation depths were determined by scanning electron microscope (SEM) images. The kinetics of the thermal oxidation of AlGaAs have been studied and

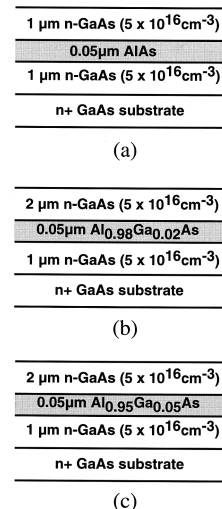


FIG. 1. Schematic cross sections of the grown structures (a) structure A, (b) structure B, and (c) structure C.

^{a)}Electronic mail: pkb@eecs.umich.edu

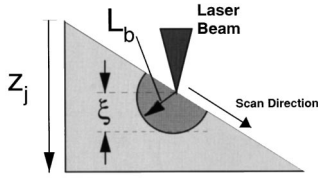


FIG. 2. Schematic showing device geometry.

published.^{16,17} Gold Schottky barriers were fabricated and a row of Schottky diodes were angle lapped for the experiment.

To perform the measurement, light from a helium–neon laser ($\lambda = 6328 \text{ \AA}$) is chopped and focused by a $50\times$ microscope objective to a spot, approximately $5 \mu\text{m}$ in diameter, onto the surface of the diode. The beam spot is approximately of the same magnitude as the diffusion length expected in n -GaAs and a factor of 10 dimensional advantage is obtained by using a beveled device structure. Therefore, for a bevel angle of 5° , as in these cases, the thickness (vertical) of the layer changes only one-tenth of the distance (horizontal) through which the scanning spot moves. The diodes were reverse biased and mounted on a three-axis micromanipulator. The photocurrent response generated was amplified using a lock-in amplifier. Current readings were taken at intervals of $1 \mu\text{m}$ along the beveled surface. The device geometry is illustrated in Fig. 2.

For an estimation of the recombination velocity near the semiconductor/oxide interface, the models of Watanabe *et al.*¹¹ and Hu *et al.*¹² were used. The total number of excess holes $\bar{\nabla}p$ in a semiconductor is given by, assuming a steady-state point excitation

$$\bar{\nabla}p = G\tau \left[1 - \frac{S}{1+S} \exp\left(-\frac{\xi}{L_b}\right) \right], \quad (1)$$

where G is the excitation, ξ is the excitation depth, and τ is the bulk lifetime. S is the reduced surface recombination velocity given by

$$S = \frac{s\tau}{L_b}, \quad (2)$$

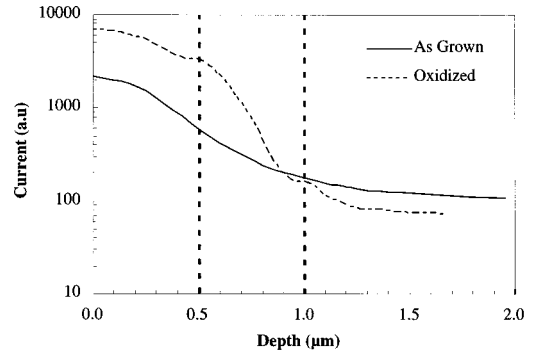
where s is the surface recombination velocity and L_b is the diffusion length of the excess holes in the bulk. It is apparent that most of the excess carriers are within the distance L_b from the excitation point and thus, for excitation depths in the order of L_b , one can assume that the change in the number of excess carriers generated is due only to surface recombination on the surface. G_{eff} incorporates this additional recombination rate introduced by recombination at the surface and is as follows:

$$G_{\text{eff}} = G \left[1 - \frac{S}{1+S} \exp\left(-\frac{\xi}{L_b}\right) \right]. \quad (3)$$

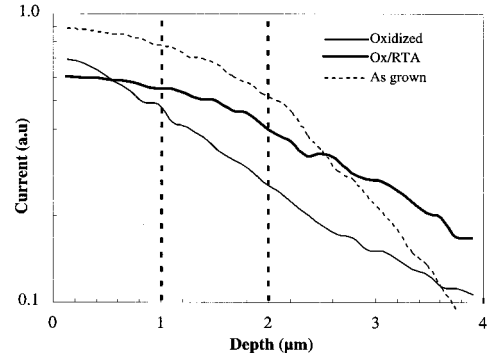
The change in G_{eff} with respect to excitation depth (for shallow excitation) is given by

$$\frac{\partial}{\partial \xi} G_{\text{eff}} = \frac{G}{L_b} \frac{S}{1+S} \exp\left(-\frac{\xi}{L_b}\right). \quad (4)$$

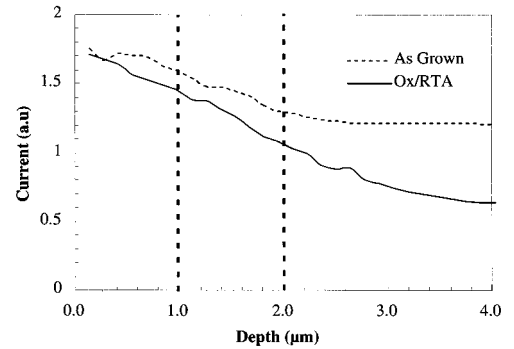
Therefore, for surface excitation, it can be shown that



(a)



(b)



(c)

FIG. 3. Typical LBIC scans for (a) structure A, (b) structure B, and (c) structure C. The vertical dashed lines mark the region near the interface.

$$\frac{\partial}{\partial \xi} G_{\text{eff}} \Big|_{\xi=0} = \frac{s}{D}, \quad (5)$$

where D is the diffusion coefficient of the excess holes. The excess carriers excited by the light beam diffuse to the Schottky junction where the electron and holes are separated and a current is generated. The light beam induced current I , a function of both ξ and z_j , is proportional to the excitation strength and decays exponentially with distance from the junction

$$I(\xi, z_j) \propto G \left[1 - \frac{S}{1+S} \exp\left(-\frac{\xi}{L_b}\right) \right] \exp\left(-\frac{z_j}{L_b}\right), \quad (6)$$

where z_j is defined as the perpendicular distance from the junction. Note that the current change can therefore also be taken as

TABLE I. Calculated minority carrier diffusion lengths and interface recombination velocities.

Structure	L_{bulk} (μm)	L_{int} (μm)		s (cm/s)	
		Before oxidation	After oxidation	Before oxidation	After oxidation
A	...	0.36	0.16	1.38 ± 10^5	3.13 ± 10^5
B	3.2	2.28	1.49	1.32 ± 10^4	1.90 ± 10^4
C	4.2	...	2.24 (RTA)	2.19 ± 10^4	3.36 ± 10^4
		3.8	2.63 (RTA)		

$$\frac{\partial}{\partial \xi} I(\xi, z_j) \Big|_{\xi=0} = \frac{s}{D}. \quad (7)$$

The exact current equation for the geometry of the device in Fig. 2, although complex, has been solved and shown to satisfy Eq. (7). It is clear from the above equations that a two-dimensional profile of the surface recombination velocity can be obtained by differentiating the current with respect to excitation depth and solving for Eq. (7).

Typical LBIC scans are shown in Figs. 3(a)–3(c). Laser scans for diodes with the oxidized and unoxidized layers are plotted on the same graph for comparison. Additional scans were performed on samples that underwent rapid thermal annealing (RTA) at 750 °C for 8 s. To avoid errors, the diffusion length in the bulk is calculated at least a diffusion length away from the Schottky junction⁸ in structures B and C where that requirement is satisfied. It is in agreement with previously measured values for the material. A reasonable value for the diffusion coefficient was taken as 5 cm²/s. The diffusion lengths near the oxide-semiconductor interface are calculated for the regions marked with the vertical dashed lines in Figs. 3(a)–3(b). They are calculated and tabulated in Table I along with the corresponding recombination velocities. Although there is a large interface state density at these interfaces, the reduction in diffusion lengths of the minority carriers due to oxidation is significantly larger for the case of oxidized AlAs. The interface recombination velocity was found to be 1.38×10^5 cm/s in that MBE-grown structure and was more than doubled after oxidation. On the other hand, the interface recombination velocities for structures B and C were found to be one order of magnitude lower and, changed less after oxidation.

These results do not come as a surprise. The improvement in structural properties and minority carrier lifetimes near the interface, with the addition of a small amount of Ga to the AlAs, have been observed before.⁶ The lateral oxidation process itself proceeds more isotropically with the presence of a small amount of gallium. It is believed that some porosity and As precipitates develop at the GaAs/Al_xO_y interface. In addition, stresses resulting from volume shrinkage during oxidation also appear to contribute to the formation of defects close to the interface.¹⁸ At this point we can only

speculate that the interface trap density, possibly resulting from the porosity and/or the strain fields, is reduced with the addition of gallium, resulting in a smaller interface recombination velocity.

In conclusion, the diffusion lengths of minority carriers and recombination velocities for the oxide/semiconductor interface were obtained using a relatively simple technique. It is found that the addition of gallium can substantially improve the recombination characteristics of the interface. The data correlate with previously presented work on the interface properties of the wet-oxidized AlAs.¹⁹ In addition to their structural and mechanical stability, multilayer structures with laterally oxidized Al-rich Al_xGa_{1-x}As exhibit improved recombination characteristics. This result is especially important when studying small aperture selectively oxidized VCSELS where leakage currents due to nonradiative recombination in and around the active region can be a limiting factor in device performance.

The authors would like to thank J. Wei for help with testing. This work was supported by COST under Grant No. MDA972-94-1-004 and ONR under Grant No. N00014-96-1-0024.

- ¹J. M. Dallesasse, N. Holonyak, Jr., A. R. Sugg, T. A. Richard, and N. El-Zein, *Appl. Phys. Lett.* **57**, 2844 (1990).
- ²G. M. Yang, M. H. MacDougal, and P. D. Dapkus, *Electron. Lett.* **31**, 886 (1995).
- ³D. L. Huffaker, T.-H. Oh, and D. G. Deppe, *IEEE Photonics Technol. Lett.* **9**, 716 (1997).
- ⁴E. I. Chen, N. Holonyak, Jr., A. R. Sugg, T. A. Richard, and N. El-Zein, *Appl. Phys. Lett.* **66**, 286 (1995).
- ⁵P. Parikh, P. Chavarkar, and U. Mishra, *Proceedings of the DRC, 1996* (unpublished), p. 134.
- ⁶K. D. Choquette, K. M. Geib, R. Hull, H. Q. Hou, K. L. Lear, H. C. Chui, B. E. Hammons, and J. A. Nevers, *Proceedings of the IEEE 9th Annual Meeting of the Lasers Electro-Optics Society, 1996* (unpublished), Vol. 1, p. 390.
- ⁷Z. Liliental-Weber, M. Li, G. S. Li, C. Chang-Hasnain, and E. R. Weber, *IEEE Conference on Semiconducting and Insulating Materials, 1996* (unpublished), p. 159.
- ⁸K. L. Ashley and J. R. Biard, *IEEE Trans. Electron Devices* **ED-14**, 429 (1967).
- ⁹J. D. Zook, *Appl. Phys. Lett.* **37**, 223 (1980).
- ¹⁰C. H. Seager, *J. Appl. Phys.* **53**, 5968 (1982).
- ¹¹M. Watanabe, G. Actor, and H. C. Gatos, *IEEE Trans. Electron Devices* **ED-24**, 1172 (1977).
- ¹²C. Hu and C. Drowley, *Solid-State Electron.* **21**, 965 (1978).
- ¹³J. Mimilla-Arroyo and J. C. Bourgoin, *J. Appl. Phys.* **55**, 2836 (1984); D. Biswas, P. R. Berger, and P. Bhattacharya, *ibid.* **65**, 2571 (1989).
- ¹⁴D. Biswas, P. R. Berger, U. Das J. E. Oh, and P. Bhattacharya, *J. Electron. Mater.* **18**, 137 (1989).
- ¹⁵M. Ochiai, G. E. Guidice, and H. Temkin, *Appl. Phys. Lett.* **68**, 1898 (1996).
- ¹⁶K. D. Choquette, K. L. Lear, R. P. Schneider, Jr., and H. C. Chui, *Proceedings of the IEEE 8th Annual Meeting of the Lasers Electro-Optics Society, 1996* (unpublished), Vol. 2, p. 412.
- ¹⁷H. Nickel, *J. Appl. Phys.* **78**, 5201 (1995).
- ¹⁸S. Guha, F. Agahi, B. Pezeshki, J. A. Kash, D. W. Kisher, and N. A. Bojarczuk, *Appl. Phys. Lett.* **68**, 906 (1996).
- ¹⁹J. A. Kash, B. Pezeshki, F. Agahi, and N. A. Bojarczuk, in *Ref. 16*, Vol. 1, p. 83.